Ecological Modelling 459 (2021) 109708

Contents lists available at ScienceDirect

Ecological Modelling

journal homepage: www.elsevier.com/locate/ecolmodel

Modeling water potential of cover crop residues on the soil surface

Carson E. Dann [a], M.L. Cabrera [a,*], R. Thapa [b,c], S. Mirsky [c], K. Tully [b], C. Reberg-Horton [d], R. Hitchcock [e], F. Morari [f]

[a] Department of Crop and Soil Sciences, University of Georgia, Athens, GA 30602, United States
[b] Department of Plant Sciences and Landscape Architecture, University of Maryland-College Park, MD 20742, United States
[c] Sustainable Agricultural Systems Laboratory, USDA-ARS, Beltsville Agricultural Research Center, Beltsville, MD 20705, United States
[d] Department of Crop and Soil Sciences, University of North Carolina, Raleigh, NC 27695, United States
[e] Agricultural and Environ. Serv. Lab., University of Georgia, Athens, GA 30602, United States
[f] Department Agronomy, Food, Natural Resources, Animals and Environment, University of Padova, Italy

ARTICLE INFO

Keywords:
Surface residue
Decomposition
Relative humidity
Crimson clover
Cereal rye

ABSTRACT

Cover crops are usually planted between cash crops to protect the soil, take up residual soil nitrate, and release nitrogen (N) to subsequent crops. Following cover crop termination, residues may remain on the soil surface, where their decomposition is largely dependent on residue temperature and water potential ($\psi_{residue}$). While it is possible to continuously measure residue temperature, continuous measurements of $\psi_{residue}$ are impractical. Thus, a practical model to estimate $\psi_{residue}$ would be useful for models of residue decomposition. To obtain data for a model of $\psi_{residue}$ for cereal rye (*Secale cereale* L.) and crimson clover (*Trifolium incarnatum* L.), we conducted studies that evaluated the effects of (1) residue stage of decomposition on water release curve; (2) relative humidity (RH) on $\psi_{residue}$; (3) soil moisture on residue gravimetric water content (θ_g); (4) precipitation on θ_g; and (5) diurnal changes in RH and temperature on $\psi_{residue}$. Results showed that water release curves for cereal rye and crimson clover changed as decomposition progressed, and that parameters for these curves could be estimated from residue lignin content. Both types of residues rewetted at a similar rate when exposed to high RH, but when rewetted by rainfall, cereal rye required a lower amount of rainfall than crimson clover to reach maximum water content. Results of these studies were used to develop, calibrate, and validate a model of $\psi_{residue}$ that requires inputs of initial water and lignin contents of the residue as well as hourly values of relative humidity, air temperature, and precipitation. Comparison of observed vs. simulated data indicated the model simulates reasonably well the observed diurnal patterns of surface $\psi_{residue}$ with R^2=0.84. Because this model requires a small set of parameters and input variables, its use may be more practical than that of more detailed models.

1. Introduction

Conservation tillage (CT), defined as any tillage and planting system that leaves a minimum of 30% of crop residues at the soil surface after planting (Soil Science Glossary Terms Committee, 2008), is often implemented to reduce soil disturbance and is considered a key component of a soil health management system (USDA-NRCS, 2017). Rotations with cover crops work synergistically with reduced tillage by contributing to crop diversity, breaking disease and pest cycles, and providing soil cover through live cover crops or residue mulches (Reicosky 2015). Combined implementation of reduced tillage and cover crops is a set of best management practices that aim to improve soil, water, and nutrient conservation.

The efficacy of a surface residue in providing these benefits is dependent on decomposition processes. Microbial activity within the soil and residue is the most significant driver of residue decomposition (Douglas and Rickman, 1992) and is largely influenced by residue characteristics and environmental conditions, in particular water availability. The availability of water in residue is often expressed in terms of water potential (ψ), an expression of the energy required to extract water relative to pure free water. Water potential is central to microbial survival and activity (Parr and Papendick, 1978) and the

Abbreviations: C, carbon; CT, conservation tillage; DI, deionized; θ_g, gravimetric water content; MPa, megapascals; N, nitrogen; RH, relative humidity; ψ, water potential; $\psi_{residue}$, residue water potential.

* Corresponding author.
E-mail address: mcabrera@uga.edu (M.L. Cabrera).

https://doi.org/10.1016/j.ecolmodel.2021.109708
Received 23 March 2021; Received in revised form 7 July 2021; Accepted 11 August 2021
Available online 30 August 2021

interaction of ψ and temperature is often the primary determinant of which microbial communities will colonize the residue substrate, as well as their growth and nutrient utilization (Magan and Lynch, 1986; Quemada et al., 1997; Singh et al., 2009). Tolerance to low and high ψ varies widely between species, though in general, higher values of ψ support greater microbial growth, enzymatic activity, and movement. Bacterial tolerances range from 0 to −10 MPa, while fungi can tolerate potentials in the range of 0 to −60 MPa (Harris, 1981). Water potential is also a primary determinant of water movement, as differences in ψ existing between the air, residue, and soil drive water movement from areas of higher potential to lower potential (Bristow et al., 1986).

The ψ of surface residue ($\psi_{residue}$) typically fluctuates due to its intermediate location between the soil and atmosphere and its continual exposure to water content fluctuations. As air temperature and/or solar radiation increase during the day, relative humidity (RH) decreases and atmospheric demand for water increases, drawing water from the residue (Bristow et al., 1986; Strømdahl, 2000; Khanchi et al., 2018; Thapa et al., 2021b). As RH increases during the evening, absorption of moisture from the air increases $\psi_{residue}$. (Snow et al., 1944; Sain and Broadbent, 1975; Manstretta and Rossi, 2015;(Thapa et al., 2021b) Precipitation as rainfall or dewfall can also increase $\psi_{residue}$ and serve as a major catalyst for making residue substrate available for degradation (Kieft, 1987; Manzoni et al., 2012; Moyano et al., 2013).

A better understanding of water dynamics in surface residue is essential for predicting residue decomposition and for improving on-farm water and nutrient management in CT systems (Bristow et al., 1986). To this end, simulation models can be utilized to describe complex mass and energy transfers, and may be effective for estimating ψ of cover crop residues on the soil surface. A $\psi_{residue}$ model that is driven by site-specific and easily-obtained environmental variables, such as temperature and RH, may be calibrated to local conditions and allow for estimation of $\psi_{residue}$ as a function of time. Several models of $\psi_{residue}$ have been developed (Bristow et al., 1986; Stroo et al., al.,1989; Iq et al., 2001; Findeling et al., 2003), but many of these models require many parameters and input data that are difficult to obtain. To our knowledge, a simple model that simulates $\psi_{residue}$ of cereal rye (*Secale cereale* L.) and crimson clover (*Trifolium incarnatum* L.) is currently unavailable. Therefore, with the overall goal of obtaining data for the development of such a model, some of the objectives of this work were to evaluate the effects of (1) residue stage of decomposition on the water release curve of cereal rye and crimson clover residues; (2) RH on $\psi_{residue}$; (3) soil moisture on θ_g; (4) precipitation on θ_g; (5) diurnal changes in RH and temperature on $\psi_{residue}$. An additional objective was to use the collected data to develop, calibrate, and validate a model to estimate $\psi_{residue}$ from hourly air temperature, RH and rainfall, variables commonly available from weather stations.

2. Materials and methods

2.1. Effect of residue decomposition stage on the water release curve

The cover crop residues used for this study were collected from sites in Georgia and Maryland, USA. In Georgia, samples were collected in April 2018 and 2019 from cover crop plots established the preceding fall on a Cecil soil (Fine, kaolinitic, thermic Typic Kanhapludults) at the J. Phil Campbell Research and Education Center near Watkinsville, GA (lat. 33° 52′ N, long. 83° 27′ W). Cereal rye (cv. 'Wrens abruzzi') and crimson clover (cv. 'A.U. Robin') were planted in October of 2017 and 2018 in adjoining strips (each 90 m x 10 m) at rates of 120 kg ha^{-1} and 30 kg ha^{-1}, respectively. The adjoining strips were planted in the same location each year and both crimson clover and cereal rye strips were allowed to grow throughout the winter. In the spring, aboveground cover crop samples were collected by clipping plants at a 2-cm height within three 0.6-m^2 quadrats. At time of sample collection in 2018, rye was in the flowering stage and 80% of the clover was in full bloom; in 2019, rye was in the flowering stage and 60% of the clover was in full bloom. The samples were dried at 65 °C for 48 h to determine dry biomass yields. After collection, cereal rye or crimson clover residues were placed into litter bags (0.56 m x 0.26 m) constructed of Sefar Nitex Synthetic Monofilament Fabric 06–1000/57 (1-mm weave, 0.65-mm thickness; Sefar AG, Heiden, CH) at dry mass equivalent rates of 7,587 kg ha^{-1} for cereal rye and 3,684 kg ha^{-1} for crimson clover, which were the respective average yields measured in 2018. In both years, cereal rye produced greater biomass yields than crimson clover. After sample collection, cover crops were terminated with a herbicide and both crimson clover and cereal rye strips were further divided into three blocks. Nine litter bags of each residue were deployed on the soil surface in respective cover crop strips, with three litter bags in each block. At 0, 2, and 4 weeks, one litter bag from each block was randomly collected and dried at 65 °C for 48 h to determine residue biomass on a dry-weight basis. Thus, the experimental design was a randomized complete block with three replications.

Detailed description on experimental design, cover crop management, and sampling protocol for the Maryland (USA) site was provided in Thapa et al. (2021b). Briefly, cover crop plots were established on Codorus (fine-loamy, mixed, active, mesic Fluvaquentic Dystrudepts) and Hatboro (fine-loamy, mixed, active, nonacid, mesic Fluvaquentic Endoaquepts) soils at the USDA's Beltsville Agricultural Research Center (39°00′51.3″N, 76°56′29.0″W, MD, USA). In one plot, red clover (*Trifolium pratense* L.) was seeded into winter wheat at the rate of 17 kg ha^{-1} on March 16, 2019. Red clover was included in this study because it is usually frost-seeded in a standing crop in MD. On a second plot, cereal rye was seeded at the rate of 134 kg ha^{-1} on October 24, 2018. Both cover crop species were terminated on May 8–9, 2019 using a combination of herbicides. Following termination, samples of cover crop residues remaining on the soil surface were collected at 0, 4, 10, and 16 weeks for red clover, and at 2, 5, and 18 weeks for cereal rye.

At both sites, dried cover crop residue samples were ground in a Model 4 Thomas-Wiley Laboratory Mill (Arthur H Thomas Co., Philadelphia, PA) and passed through a 2-mm sieve. Residue crude protein (CP), fat, non-fibrous carbohydrates, acid detergent fiber (ADF), neutral detergent fiber (NDF), lignin, ash, cellulose and hemicellulose were estimated by near-infrared spectroscopy (NIRS), which was previously calibrated with detergent fiber analyses (Table 1; Van Soest, 1963a, 1963b; Woodruff et al., 2018).

Water release curves were developed for the residue samples collected at different stages of decomposition. For that purpose, Ziploc bags were filled with 10 g residue using an equal ratio of leaves and stems, and varying volumes of deionized (DI) water were added to obtain θ_g values ranging from 0.1 to 3 g H_2O g^{-1} dry matter. Following equilibration for 12 h at 2 °C, subsamples were removed in triplicate from each bag, placed in sample cups, and $\psi_{residue}$ was measured using a WP4-C Dewpoint Potentiameter (Meter Group Inc., Pullman, WA), which was calibrated with certified solutions. The contents of each sample cup were then immediately dried at 65 °C for 48 h to determine θ_g. Nonlinear regression was used to fit the following equation to the data:

$$\psi_{residue} = a \cdot (\text{residue } \theta_g)^b \quad (1)$$

where, $\psi_{residue}$ is the residue water potential (MPa), residue θ_g is the residue gravimetric water content (g H_2O g^{-1} dry matter), and '*a*' and '*b*' are regression parameters.

2.2. Effect of air relative humidity (RH) on residue water potential ($\psi_{residue}$)

Residues of cereal rye and crimson clover collected in Georgia at 0 weeks were used for this study. A constant-humidity chamber was constructed using a plastic container (36 cm L, 23 cm W, 14 cm H) placed within a Precision Model 815 incubator (Precision Scientific,

Table 1
Results of the near infra-red reflectance spectroscopy (NIRS) analyses and parameters "a" and "b" of the residue water release model fit (Eq.[1]) for cereal rye, crimson clover, and red clover residues collected at different stages of decomposition in Georgia and Maryland, USA.

Residue	State	Weeks	% N[†]	% LIG[†]	% CARB[†]	% CELL[†]	Parameter a	Parameter b	RMSE[‡]
					——% of Total C——				
Cereal rye	GA	0	0.77	8.74	22.54	68.72	−3.991	−1.206	5.4
	GA	2	0.71	11.04	15.46	73.50	−1.137	−1.632	1.8
	GA	4	0.73	12.82	12.11	75.07	−0.418	−2.056	1.8
Cereal rye	MD[§]	2	0.96	7.53	21.98	70.49	−3.469	−1.177	3.8
	MD	5	0.99	8.95	22.27	68.78	−1.997	−1.321	4.0
	MD	18	1.19	11.17	24.52	64.31	−1.−75	−1.555	3.4
Crimson clover	GA	0	2.71	4.05	56.00	39.95	−6.648	−1.058	2.4
	GA	2	2.32	7.05	42.52	50.43	−3.631	−1.148	6.7
	GA	4	2.23	8.92	23.73	67.35	−2.406	−1.403	2.2
Red clover	MD	0	2.58	5.62	53.79	40.59	−4.547	−1.179	1.2
	MD	4	2.61	10.27	35.96	53.77	−2.290	−1.477	4.4
	MD	10	2.89	12.78	34.17	53.05	−0.679	−2.165	3.7
	MD	16	3.02	14.01	36.35	49.64	−0.685	−2.039	3.3

[†] Values are replicate averages for each site-days of decomposition. N, nitrogen; C, carbon; LIG, lignin; CARB, soluble carbohydrates; CELL, cellulose + hemicellulose.
[‡] RMSE is the root mean squared error of the model.
[§] Data for the MD site were obtained from Thapa et al. (2021b).

Winchester, VA) set at 30 °C. Vacuum regulated by a Dwyer VFB-66 flowmeter (Dwyer, Michigan City, IN) was used to draw air through the chamber at 0.2 L min^{-1}. Air temperature and RH within the chamber and within the incubator were monitored and recorded at 5-min intervals with HMP155A probes connected to a CR1000 datalogger (Campbell Scientific, Logan, UT).

To study the rate of residue rewetting at high RH, air delivered to the chamber was humidified to 93% RH by bubbling it through DI water, and WP4-C sample cups were filled with 0.5 g of air-dry cereal rye (0.03 g H_2O g^{-1} dry matter) or crimson clover (0.04 g H_2O g^{-1} dry matter) residue cut into 3-cm pieces. Sample cups were removed in triplicate every 0.5 h for the first 2 h, and every 2 h thereafter up to 24 h to measure $\psi_{residue}$ using a WP4-C Dewpoint Potentiameter.

To study the rate of residue drying at low RH, lab air at 33% RH was circulated through the chamber. Cereal rye and crimson clover residues were prepared by saturating them with DI water and allowing them to equilibrate at 2 °C for 12 h. Initial θ_g of cereal rye and crimson clover residues were 3.56 g H_2O g^{-1} dry matter and 4.05 g H_2O g^{-1} dry matter, respectively. After determining residue θ_g, a wet-weight equivalent of 0.5 g oven-dry residue was placed in WP4-C sample cups, which were then placed in the drying chamber. The residues cups were removed from the chamber in triplicate every 1 to 3 h over a 24-h period and the $\psi_{residue}$ was measured with a WP4-C Dewpoint Potentiameter.

2.3. Effect of soil water content on residue water content (θ_g)

To study changes in $\psi_{residue}$ when dry residue was placed on wet soil, air-dry soil from the Georgia site was packed into aluminum moisture cans (8 cm ID, 5 cm H) at a bulk density of 1.4 g cm^{-3}, and DI water was added to each can to bring the soil water content to −0.03 MPa; the cans were sealed and soil moisture was allowed to equilibrate for 48 h. Crimson clover and cereal rye residue collected at 0 weeks from the Georgia site were dried to 0.1 g H_2O g^{-1} dry matter, cut to a length of 3.5 cm, and surface-applied on wet soil to each can at a rate corresponding to 7,587 kg ha^{-1} for cereal rye and 3,684 kg ha^{-1} for crimson clover. These rates produced a mulch layer of 2 to 3 cm on the soil surface, with a lower layer in direct contact with the soil, and with upper layers that did not contact the soil. In addition, cans containing only residue served as controls to account for the effect of RH within the incubator. Cans were placed within a Precision Model 815 incubator set at 22 °C. Air temperature and RH within the incubator were measured and recorded at 5-min intervals with a HMP155A probe connected to a CR1000 datalogger. Two cans per residue type and two controls were removed from the incubator at 0.2, 0.5, 1, 3, 5, 8, 12, 15, and 19 h. Residues were removed from the soil surface of each can and sealed in a Ziploc bag, after which $\psi_{residue}$ was measured in duplicate with a WP4-C Dewpoint Potentiameter.

To study changes in the $\psi_{residue}$ of wet residues in contact with low-moisture soil, the procedure described above was modified in the following ways: Soil was air-dried under laboratory conditions until reaching a target of −1.5 MPa (permanent wilting point; Stott et al., 1986), and then packed into cans at a bulk density of 1.4 g cm^{-3}. A Ziploc bag was filled with air- dry residues of crimson clover or cereal rye, and DI water added to obtain a target residue water content of 2 g H_2O g^{-1} dry matter· Following equilibration, wetted residues (1.44 g H_2O g^{-1}dry matter for rye and 1.97 g H_2O g^{-1} dry matter for crimson clover) were applied to each can and cans were sealed with lids to exclude the effect of the atmosphere on residue drying while in the incubator. Two cans per residue type were removed from the incubator at 0.2, 0.5, 1, 3, 5, 8, 12, 15, and 19 h., and the $\psi_{residue}$ was measured in triplicate with a WP4-C Dewpoint Potentiameter.

2.4. Effect of precipitation on residue water content (θ_g)

To determine the response of residue θ_g to rainfall, an indoor rainfall simulation study was conducted with residues collected at 0 weeks from the Georgia site. Two simulators were installed at a height of 2 m from the ground, with each simulator consisting of 256 hypodermic needles (23 gage by 25.4 mm) uniformly spaced on a 0.09-m^2 acrylic panel. A peristaltic pump connected to plastic tubing delivered DI water to each simulator at a flow rate of 50 mm h^{-1}, which generated 10.4-mg droplets (Kissel et al., 2004). Air-dry crimson clover (θ_g = 0.03 g H_2O g^{-1} dry matter) or cereal rye residue (θ_g = 0.05 g H_2O g^{-1} dry matter) was placed on 0.07-m^2 metal sieve trays at the dry-weight equivalent of 3000 or 6,000 kg ha^{-1}. There were three replications per residue rate and two residue rates per residue species. Trays were placed directly on the ground below simulators and elevated 5 cm from the floor to allow water drainage from the tray. Simulated rain was allowed to fall on the trays in 5-min intervals, corresponding to 4.17 mm of rainfall per interval. Between intervals, trays were vigorously shaken to remove surface water on the residue and then weighed. Trays were subsequently placed back under the simulators and rainfall was resumed. Simulation continued in this manner until a stabilization in weight was obtained, which was determined by a change in tray weight < 1% between two consecutive rainfall intervals. Residue θ_g was then regressed against rainfall amount (mm). During the course of rainfall simulations, air temperature within the lab fluctuated between 21 and 22 °C.

2.5. Effect of diurnal changes in RH and temperature on residue water potential

Six field studies were conducted at the Georgia site to measure diurnal fluctuations in $\psi_{residue}$ as affected by RH and air temperature (June 8, August 15–16, and September 5, 2018; July 24–25, August 28–29, and September 11–12, 2019). The dry-weight equivalent of 0.5 g of air-dry crimson clover or cereal rye residue (collected at 0 weeks from the Georgia site) was added to WP4-C sample cups and placed on top of cereal rye or crimson clover residue cover at the Georgia site strips. A subset of the samples was exposed to dew and a subset was shielded from dew by using small, plastic "tents" placed right above the samples. Samples of each residue species were collected in triplicate every 3 to 4 h during each study, and $\psi_{residue}$ was measured with a WP4-C Dewpoint Potentiameter.

2.6. Statistical analyses

The statistical software JMP v. 15 (SAS Institute Inc., 2019) was used to determine parameters "a" and "b" of the nonlinear model for the water release curves. Subsequently, stepwise regression in SAS software version 9.4 (SAS Institute Inc., 2015) was used to regress the parameters of the nonlinear model for both cereal rye and crimson clover against residue N, CARB, CELL, and LIG. These variables were considered because they are continuously simulated in the decomposition model to which the model of $\psi_{residue}$ will be coupled, and therefore could be used (if found significant) at any stage in the decomposition to estimate the parameters of the moisture release curve.

The sum of squares errors obtained when fitting the nonlinear model to the water release curves were used to perform a conditional error test to determine if the nonlinear models fitted to the water release curve for each cover crop residue at each decomposition stage were significantly different from each other (Milliken and DeBruin, 1978). For that purpose, we conducted pairwise comparisons of the water release curves fitted to a given crop residue at different stages of decomposition. The null hypothesis (Ho) in the conditional error test was that a single model could be used to describe two different datasets (two water release curves from different decomposition stages); the alternative hypothesis (Ha) was that two different model were needed to describe the two datasets. To obtain the sum of squares residual under Ho (SSres(Ho)), we fitted a single model to the two datasets, and to obtain the sum of squares residual under Ha (SSres(Ha)), we fitted individual models to each of the two datasets and added the two sum of squares residuals. To calculate the sum of squares residuals due to deviations from Ho (SSres (devHo)), we subtracted SSres(Ha)) from SSres(Ho)). Similarly, the degrees of freedom (df) for SSres(devHo)) were calculated by subtracting the degress of freedom of SSres(Ha) from the degrees of freedom of SSres (Ho)). Finally, an F test was performed with SSres(devHo))/df in the numerator and SSres(Ha)/df in the denominator. If the F value was greater than the table F value with corresponding degrees of freedom at $p = 0.05$, Ho was rejected and the conclusion was reached that the two models were significantly different.

We used PROC MIXED in SAS v. 9.4 to analyze the effect of cover crop species (rye or crimson clover) on $\psi_{residue}$ at different hours of rewetting (under constant high RH), or on $\psi_{residue}$ at different hours of drying (under constant low RH). The analysis considered residue type and time as fixed factors, and replication as a random factor. PROC MIXED was also used to separately analyze the effect of contact time with wet or dry soil on $\psi_{residue}$. Time was considered a fixed factor and replication a random factor.

To analyze the effect of simulated rain amounts on θ_g of cereal rye or crimson clover residue at two rates (3000 or 6,000 kg ha^{-1}), we used PROC MIXED considering dry matter rate and rain amount as fixed factors, and replication as a random factor, with compound symmetry as the covariance structure. The θ_g measured at different amounts of rain was considered a repeated measurement. A nonlinear regression model was fitted to the data of θ_g versus simulated rain amount using JMP V. 15.

2.7. Model development

We developed a model simulating $\psi_{residue}$ of surface cover crop residues that is driven by hourly data commonly monitored by weather stations, namely RH, air temperature, and precipitation measured at a 2-m height. A stock variable in the model represents residue θ_g, which changes based on inward and outward flows (Fig. S1). During simulation, water moves into the residue according to differences in ψ between the residue and atmosphere, and water moves out of the residue according to residue θ_g, RH, and ambient temperature. The residue can also gain water via dewfall and precipitation.

2.8. Model calibration

Model parameters were calibrated manually using data from a 41-h field study described in Section 2.5, which was conducted on August 15–16, 2018. Statistical tools used for calibration included root mean square error (RMSE), Nash-Sutcliffe Efficiency (NSE), and R^2 values for observed vs. simulated data (Nash and Sutcliffe, 1970; Addiscott and Whitmore, 1987; Quemada and Cabrera, 1995b). In general, a statistically satisfactory model simulation results in a low RMSE and an R^2 value greater than 0.5. NSE values between 0 and 1 are generally indicative of acceptable model performance (Moriasi et al., 2007).

2.9. Model validation

Model performance was validated with five of the six diurnal studies described in Section 2.5 (June 8 and September 5, 2018; July 24–25, August 28–29, and September 11–12, 2019). The same statistical tools used for calibration were used for model validation.

3. Results and discussion

3.1. Effect of residue decomposition on the water release curve

The water potential of residues has three main components: gravitational potential, matric potential, and osmotic potential, with the latter two being the most important for surface residues. The matric potential represents the capacity of the residue to retain water due to adsorption and capillary effects caused by physical characteristics such as pore sizes as well as chemical characteristics. The osmotic potential represents the capacity of the residue to retain water due to the presence of solutes in the water (Young and Sisson, 2002). Fitting the nonlinear model in Eq.[1] to $\psi_{residue}$ versus residue θ_g for the different cover crop residues at different decomposition stages yielded R^2 values ranging from 0.80 to 0.99 (Fig. 1). With progressive decomposition, residues held less water at a given $\psi_{residue}$ and more readily approached saturation ($\psi_{residue} = 0$ MPa) as residue θ_g increased.

The conditional error test performed for pairwise comparisons of models indicated that within each residue type, the water release models were significantly different as decomposition progressed (Table 2). These results are in agreement with findings of several studies (Coppens et al., 2007; Findeling et al., 2007; Dunlop et al., 2016; Khanchi et al., 2018; Thapa et al., 2021b), and are due in part to the leaching of solutes as residues decompose, which decreases the osmotic potential and progressively shifts the primary component of $\psi_{residue}$ to the matric potential (Myrold et al., 1981). In addition, porosity of residue tissues increases as cellulose and hemicellulose are enzymatically degraded over time, allowing water to be more readily gained and lost by plant tissue and altering the maximum water content possible (Maloney and Paulpuro, 1999; Quemada and Cabrera, 2002; Iqbal et al., 2013).

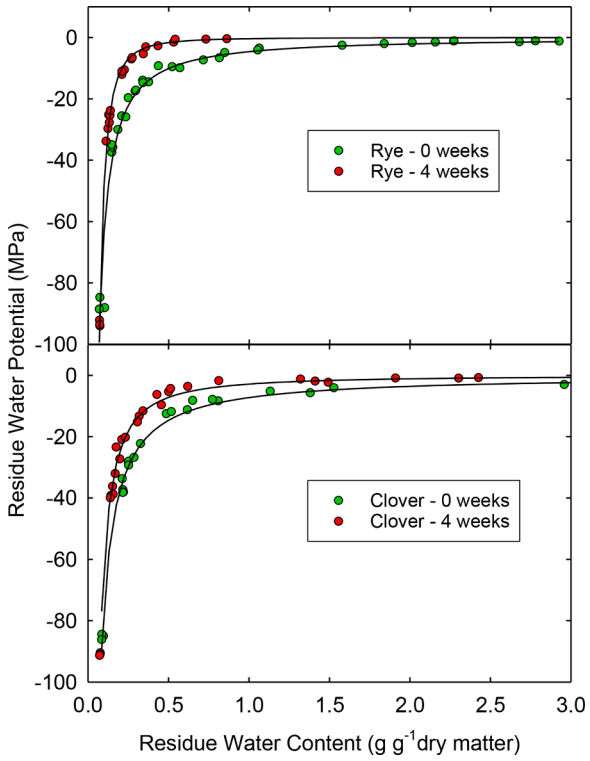

Fig. 1. Water potential of cereal rye and crimson clover residues as a function of water content at 0 and 4 weeks of decomposition in a Georgia study.

The stepwise regression of parameters 'a' and 'b' on residue N, CARB, CELL, and LIGN contents showed that LIGN was the only significant variable that could be used to estimate both parameters of the water release curve (Fig. 2) Soluble carbohydrates are decomposed first from the residues, which increases lignin concentration as decomposition progresses (Table 2). As lignin concentrations in the residues increased, parameter "a" increased (less negative) whereas parameter "b" decreased (more negative). A single regression to estimate model parameters for all residues is convenient because it does not require the user to identify the type of cover crop residue in order to determine the regression model to be used.

3.2. Effect of air relative humidity (RH) on residue water potential ($\psi_{residue}$)

When studying the influence of high RH on residue rewetting, temperature within the chamber fluctuated between 27.8 and 28.5 °C, and RH ranged from 88 to 94%. The relationship of $\psi_{residue}$ vs. time displayed an exponential trend with $\psi_{residue}$ changing most drastically within the first 5 h of rewetting, and approaching equilibrium with air ψ (ψ_{air}) after 15 h (Fig. 3a).

Cereal rye $\psi_{residue}$ increased from −135.4 MPa (0.06 g H_2O g^{-1} dry matter) −11.7 MPa (0.42 g H_2O g^{-1} dry matter) crimson clover $\psi_{residue}$ increased from −103.5 MPa (0.08 g H_2O g^{-1} dry matter) to −11.4 MPa (0.60 g H_2O g^{-1} dry matter) (Fig. 3a). The relatively fast increase in $\psi_{residue}$ observed agrees with the rapid increases in ψ observed overnight by Cassity-Duffey et al. (2015) in a field study of broiler litter applied to the soil surface, which suggests that RH is one of the main controlling factors in rewetting surface residues.

The analysis of variance showed a significant ($p<0.0001$) residue type x time interaction effect on residue rewetting, which was due to differences in $\psi_{residue}$ between cereal rye and crimson clover residues at 0 and 0.5 h ($p<0.001$). These were mainly caused by slightly different initial amounts of θ_g in the residues. Despite notable differences in residue chemistry (Table 1), the rewetting rates of cereal rye and crimson clover residues were similar (after 0.5 h) when placed under identical conditions of RH and temperature (Fig. 3a). Moisture absorption by plant material in contact with air is a physical phenomenon involving Van der Waal forces between water molecules and hydroxyl groups of residue cell walls. As RH exceeds 70%, a significant amount of water uptake is not actually sorbed but held loosely within residue pores as a result of capillary condensation (Strømdahl, 2000).

When studying the influence of low RH on residue drying, temperature and RH within the chamber fluctuated between 29.4 and 30.4 °C, and between 31 and 33%, respectively. Cereal rye $\psi_{residue}$ decreased from −0.6 MPa (2.93 g H_2Og^{-1} dry matter) to −153.9 MPa (0.05 g H_2O g^{-1} dry matter) crimson clover $\psi_{residue}$ decreased from −0.7 MPa (3.06 g H_2O g^{-1} dry matter) to −147.9 MPa (0.06 g H_2O g^{-1} dry matter) (Fig. 3b). The $\psi_{residue}$ displayed a logistic trend with time, with $\psi_{residue}$ changing at a much slower rate than that observed in the rewetting study.

The analysis of variance showed a significant ($p<0.07$) residue type x time interaction effect on residue drying, which was due to differences in $\psi_{residue}$ between crimson clover and cereal rye residues at more than 15 h of drying ($p<0.05$; Fig. 3b). At 15 h, the water potential was lower than −100 MPa at which very little to no decomposition is expected (Thapa et al., 2021b). Therefore, a single model was used for changes in $\psi_{residue}$ as residue dries. Also, because field observations (presented below)

Table 2
Sum of square errors for null and alternative hypothesis for pairwise comparisons of models of moisture release curves for cover crop residues of cereal rye and crimson clover collected in GA, and for cover crop residues of cereal rye and red clover collected in MD. The models were compared using the conditional error principle.

Residue	State	Comparison	SSEHo	dfHo	SSEHa	dfHa	F
Rye	GA	0 vs 2 wk	2317	55	946	52	25**†
		0 vs 4 wk	3477	55	942	52	46**
		2 vs 4 wk	318	46	138	44	29**
Rye	MD	2 vs 5 wk	3535	183	2848	181	22**
		2 vs 18 wk	2936	102	1324	100	61**
		5 vs 18 wk	2424	159	324	157	65**
Crimson Clover	GA	0 vs 2 wk	3447	52	1275	50	43**
		0 vs 4 wk	1418	52	260	50	111**
		2 vs 4 wk	1917	52	1258	50	13**
Red Clover	MD	0 vs 4 wk	3870	226	3442	224	14**
		0 vs 10 wk	3752	227	2445	225	60**
		0 vs 16 wk	3205	182	1530	180	98**
		4 vs 10 wk	7958	357	5753	355	68**
		4 vs 16 wk	6639	311	4838	309	58**
		10 vs 16 wk	6151	312	3841	311	187**

† indicates significant at $p<0.01$.

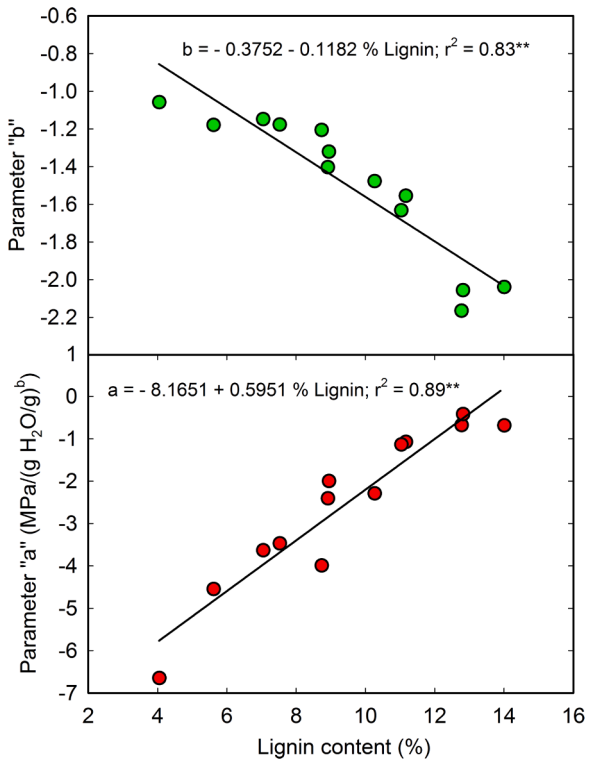

Fig. 2. Parameters of equation describing water release curve ($\psi_{residue} = a \cdot (\text{residue } \theta_g)^b$ as a function of residue lignin content at different stages of decomposition for cereal rye and crimson clover residues (together).

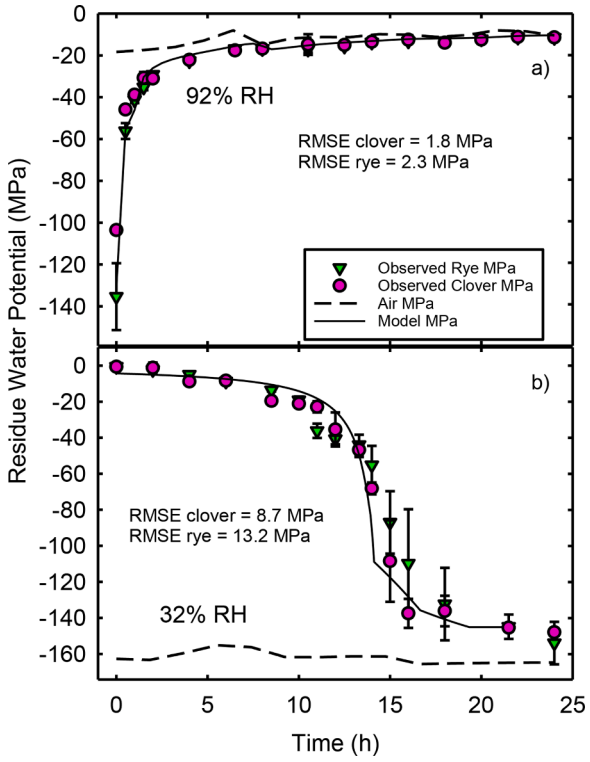

Fig. 3. Changes in the water potential (MPa) of cereal rye and crimson clover residues over time (h) in a laboratory study at 30 °C and (a) 92% RH or (b) 32% RH. The full lines represent modeled results.

indicate a much faster drying of residues, these results suggest that other factors in addition to RH control residue drying under field conditions. In the modeling description below, temperature is used as a variable involved in residue drying.

3.3. Effect of soil water content on residue water content (θ_g)

When cereal rye residue at 0.1 g H_2O g^{-1} dry matter (−69 MPa) was placed in contact with wet soil at −0.03 MPa (0.28 g H_2O g^{-1} dry matter), the $\psi_{residue}$ increased significantly from −67 MPa to −38 MPa in 3 h, and from −38 MPa to a maximum of −25 MPa after 18 h ($p<0.05$). Similarly, for crimson clover the $\psi_{residue}$ increased significantly from −68 MPa to −40 MPa in 3 h, and from −40 MPa to a maximum of −28 MPa after 18 h ($p<0.05$). This corresponds to average increases in residue θ_g of only 15% for cereal rye and 25% for crimson clover. According to the temperature and water potential adjustment factor developed by (Thapa et al., 2021a; the rate of residue decomposition at average conditions of −26 MPa (the average water potential at which the residues equilibrated in our study) and 22 °C would be less than 0.1% of the maximum possible. Thus, we can conclude that residue rewetting from soil under our conditions would have a negligible effect on residue decomposition when compared to the effects of RH (Sain and Broadbent, 1975) and rainfall. Consequently, we decided to omit the effect of residue rewetting from soil in the $\psi_{residue}$ model, which served to simplify the model and improve its utility for users without access to hourly soil moisture data for their site or a specific water release curve for their soil.

When wet residue was placed in contact with dry soil at −1.5 MPa, we observed a small but significant ($p<0.05$) increase in rye residue θ_g from 1.44 to 1.56 g H_2O g^{-1} dry matter (increase in $\psi_{residue}$ from −2.8 to −2.1 MPa), and a small but significant ($p<0.05$) increase in crimson clover residue θ_g from 1.97 to 2.08 g H_2O g^{-1} dry matter (increase in $\psi_{residue}$ from −2.8 to −1.6 MPa). These observed small increases in residue θ_g were likely because the wet residues at time 0 still had ψ lower than that of the dry soil at time 0 (i.e., −2.8 MPa for wet residues vs. −1.5 MPa for dry soil). As a result, we observed no drying of wet residues even when placed in contact with the dry soil.

3.4. Effect of precipitation on residue water content (θ_g)

The θ_g of both residue species increased rapidly with the first 6 mm of rainfall, after which gains in residue moisture progressively diminished as residues approached maximum water content (Fig 4). This trend was likewise observed by Manstretta and Rossi (2015) when developing a relationship between rainfall and water content of corn stalk residue. Cereal rye residue did not attain a θ_g of 3 g H_2O g^{-1} dry matter until receiving ~25 mm of rainfall (Fig. 4a), whereas crimson clover residue θ_g reached that value after only 12 mm of rainfall (Fig. 4b).

This disparity is likely a result of differences in the residue morphology and chemistry. Crimson clover provided a larger surface area for rainfall interception due to its wider leaves and greater leaf:stem ratio, whereas the surface area of cereal rye was lower due to its characteristically thinner leaves and lower leaf:stem ratio (Barnett et al., 2002). Such morphological and anatomical differences existing between plant residues are likely crucial for determining a residue's propensity to undergo water recharge during precipitation events (Shane et al., 2000; Iqbal et al., 2013). A greater proportion of stems in the cereal rye treatments likely inhibited residue water uptake due to a greater concentration of lignin in stems than in leaves and thus a greater hydrophobicity of stem tissues (Quemada and Cabrera, 1995a; Horwath, 2015, Thapa et al., 2021b). In addition to lignin concentration, Quemada and Cabrera (2002) suggested that the greater water absorption and retention properties of crimson clover residues are largely determined by a greater concentration of soluble constituents (i.e. greater osmotic potential), and thus proposed soluble carbohydrate content as a

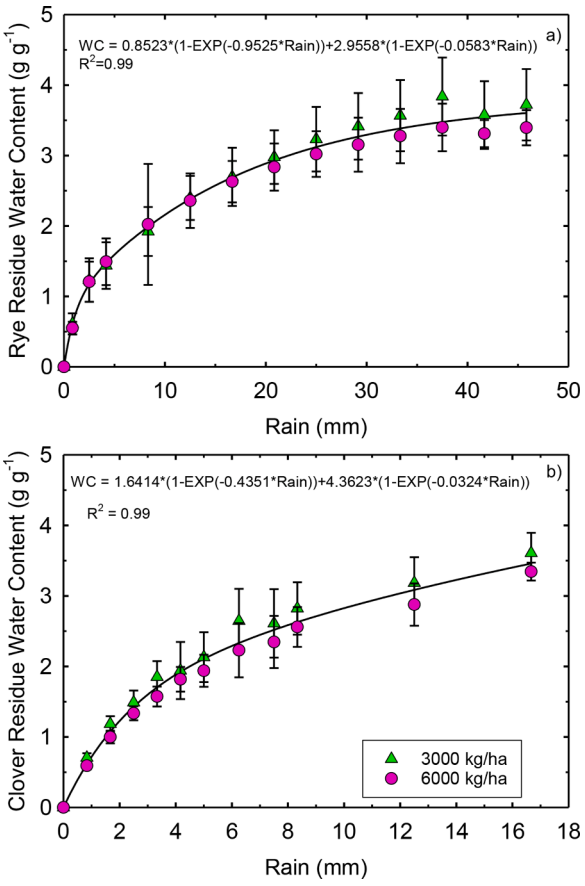

Fig. 4. Effect of simulated rainfall on residue gravimetric water content at two biomass rates (3000 and 6000 kg dry matter ha^{-1}) for cereal rye (a) and crimson clover (b) residues.

good predictor of a residue's maximum water content. It should be noted that a residue's propensity to undergo water recharge also changes significantly with progressive decomposition. The increased porosity of decomposed residues leads to a more rapid absorption of rainwater and attainment of saturation, followed by the dripping and infiltration of water into the soil. The rate of water evaporation from the residue is also increased with increased porosity (Coppens et al., 2006). Thus, decomposition stage is likely to have a significant effect on a residue layer's interception and retention of rainwater.

For cereal rye residue, we found a significant interaction ($p<0.05$) of dry matter rate x rain amount on residue θ_g, which was due to small differences in θ_g at large rain amounts. At rain > 33 mm, which corresponds to $\theta_g > 3.0$ g H_2O g^{-1} dry matter, the θ_g of rye residue was about 0.25 g H_2O g^{-1} dry matter greater at 3,000 kg ha^{-1} than at 6,000 kg ha^{-1}. According to the water release curve for cereal rye (0 week, Table 1) an increase in θ_g from 3 to 3.25 g H_2O g^{-1} dry matter would increase $\psi_{residue}$ from −1.06 to −0.96 MPa, which in turn would increase the rate of residue decomposition by less than 2.5% at 20 °C as per the adjustment factor developed by Thapa et al., 2021a; For clover residue, dry matter rate and the dry matter rate x rain amount interaction had no significant effect on θ_g. Given the lack of effect of dry matter rate on crimson clover residue θ_g and the low effect of dry matter rate on cereal rye θ_g, a single nonlinear regression model was fit to data from both dry matter rates for each residue type (Fig. 4). The regressions obtained were later incorporated into the $\psi_{residue}$ model, as described below, to estimate changes in θ_g of surface residues due to a rain event.

In general, our results showed similar wetting patterns at the two dry matter rates for each residue type (Fig. 4a, b). This could be attributed to differences in surface area between the two dry matter rates, which led to different amounts of rain interception and throughfall. We measured about twice as much throughfall at 3000 kg ha^{-1} than at 6000 kg ha^{-1} (data not shown) and as a result, a given rain amount produced about the same θ_g at both dry matter rates.

3.5. Effect of diurnal changes in RH and temperature on residue water potential ($\psi_{residue}$)

As described above, a total of six studies were conducted at the Georgia site from 2018–2019 to measure fluctuations in $\psi_{residue}$ under field conditions, and to assess the effect of diurnal changes in RH and temperature. Results for five of those studies are shown in Figs. 5 and 6. Average temperature for these studies ranged from 17 to 32 °C and average RH fluctuated from 39 to 97%. Fluctuations in $\psi_{residue}$ corresponding to diurnal fluctuations in RH were observed in each of these studies.

Maximum $\psi_{residue}$ measurements were recorded at times of peak RH (about 6 am), while minimum values were recorded at times of lowest RH (about 3:30 pm). The average $\psi_{residue}$ of residue shielded from dew fluctuated diurnally from −16.3 MPa to −210.5 MPa for cereal rye, and from −17.2 MPa to −190.6 MPa for crimson clover. Such drastic changes in $\psi_{residue}$ closely mirror diurnal changes in ψ_{air}. As air temperature and solar radiation increase during the day, RH decreases and atmospheric demand for water increases, drawing water from the residue. Likewise, as RH increases during the night, the dried residue absorbs water from the atmosphere (Parr and Papendick, 1978; Bristow et al., 1986; Cassity-Duffey et al., 2015; Manstretta and Rossi, 2015; Khanchi et al., 2018; Thapa et al., 2021b). In agreement with findings from our previously described lab study of RH and $\psi_{residue}$, the wetting and drying behavior of cereal rye and crimson clover residue was very similar when residues were exposed to the same conditions of RH and temperature in the field (Figs. 5 and 6).

A subset of residue samples was exposed to dewfall in four of the six diurnal studies and removed in triplicate at hours of peak RH. An average deposition of 0.23 mm of dew was estimated across the four studies ($N = 14$). This aligns with the findings of Cassity-Duffey et al. (2015), who recorded an average of 0.2 mm of dew daily in a microlysimeter study under similar conditions. Dew deposition increased θ_g of residues by averages of 0.49 g H_2O g^{-1} dry matter (10.4 MPa, std dev = 1.4 MPa) for cereal rye and 0.86 g H_2O g^{-1} dry matter (11.4 MPa, std dev = 2.1 MPa) for crimson clover. The increase in residue θ_g following dewfall was consistently greater for clover than for cereal rye across all four studies, aligning with results from the rainfall simulation study. Large increases in θ_g due to dew were recorded at RH values as low as 85% at a 2-m height.

3.6. Model development

The developed model uses a small number of variables (Table S1) and a small set of inputs, namely initial water and lignin contents of the residue, and hourly RH, air temperature, and precipitation. The residue lignin content is used to estimate the parameters of the water release curve for the residue, as shown in Fig. 2. RH and temperature are used to calculate air WP (ψ_{air}) using the following equation:

$$\psi_{air} = \frac{R\cdot(T+273.15)}{V}\cdot\frac{ln(RH)\cdot 1\ MPa}{1,000,000\ Pa} \quad (2)$$

where, R is the universal gas constant (8.314 $J\,K^{-1}\,mol^{-1}$), T is the air temperature at 2-m height (°C), V is the partial molar volume of water (1.8×10^{-5} $m^3\,mol^{-1}$), and RH is the relative humidity of air at 2-m height expressed as a fraction (0–1). Transfer of water from the air to the residue occurs with a positive change in RH between timesteps (RH_t-$RH_{(t-1)}$). The transfer of water from air to surface residues (i.e., residue rewetting) usually occurs during nighttime and early morning hours (when the RH of the air increases) and is driven by the $\psi_{gradient}$ between

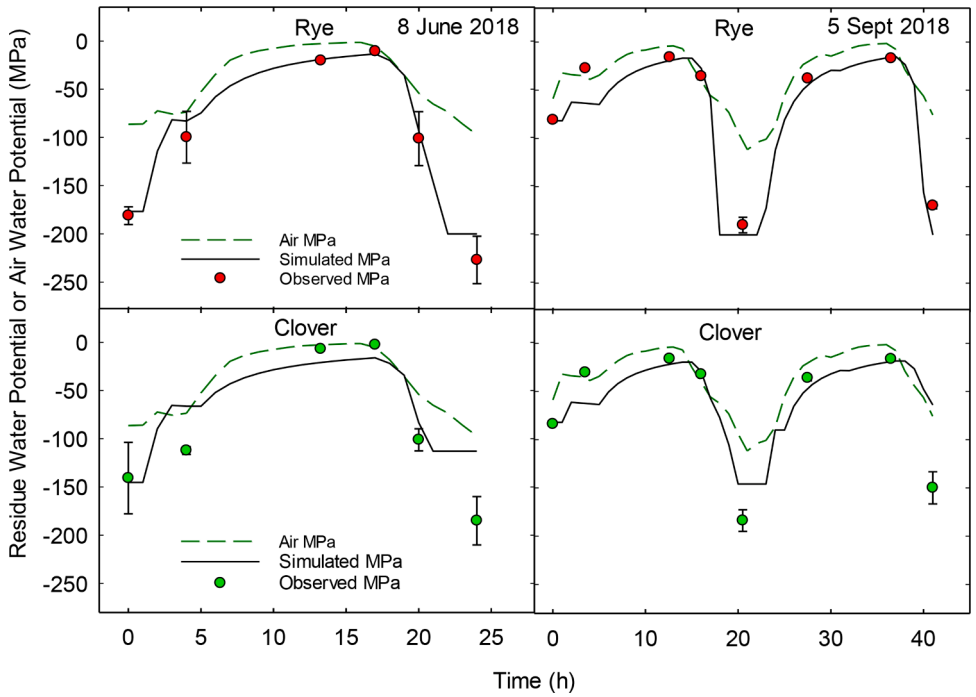

Fig. 5. Observed air water potential (ψ_{air}) and simulated and observed residue water potentials ($\psi_{residue}$) for cereal rye and crimson clover residues shielded from dew on 8 June and 5 September 2018.

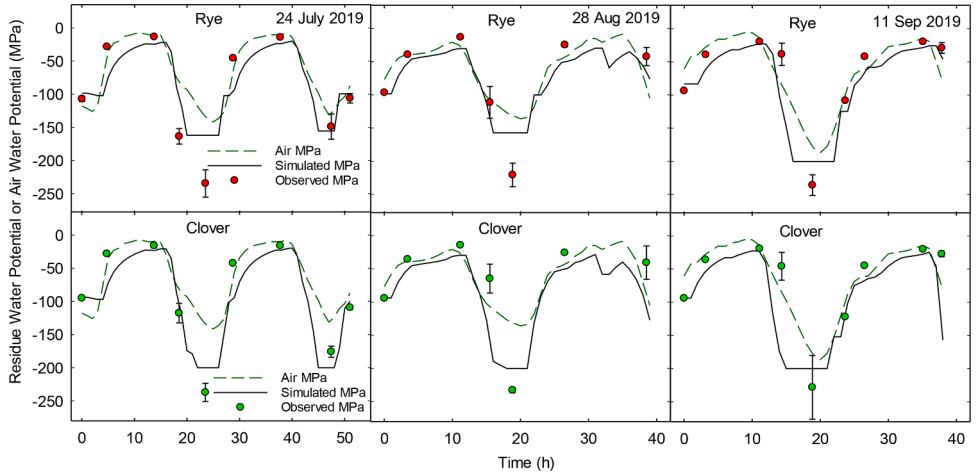

Fig. 6. Observed air water potential (ψ_{air}) and simulated and observed residue water potentials ($\psi_{residue}$) for cereal rye and crimson clover residues shielded from dew on 24 July, 28 August, and 11 September 2019.

surface residues and the air above it. The rate of residue rewetting due to positive change in RH and $\psi_{gradient}$ is modeled using the following equations:

$$\frac{\Delta \text{residue } \theta_g}{\Delta t} = k_1 \cdot \psi_{gradient} \tag{3}$$

where, $\frac{\Delta \text{residue } \theta_g}{\Delta t}$ is the rate of residue rewetting and is expressed as per unit gain in residue θ_g per unit change in time (g H_2O g^{-1} dry matter h^{-1}), Δt is the change in time (h), k_1 is a rate constant (g H_2O g^{-1} dry matter h^{-1} MPa^{-1}), and $\psi_{gradient}$ is the ψ gradient between air and surface residues (MPa) The rate constant k_1 described below was used as the initial value for the model based on results from the lab study on rewetting residue. The value of k1 is greater for clover than for rye because of the differences in initial water content, as described above.

$$k_1 = \begin{cases} 0.0038,\ \Delta RH > 0\ (AND)\ \psi_{gradient} < 30 \\ 0.002,\ clover\ (\text{AND})\ \Delta RH > 0\ (AND)\ \psi_{gradient} > 30 \\ 0.001,\ rye\ (\text{AND})\ \Delta RH > 0\ (AND)\ \psi_{gradient} > 30 \\ 0,\ \Delta RH \le 0 \end{cases} \tag{4}$$

The transfer of water from surface residues to air via evaporation (i.e., residue drying) occurs during daytime hours when the RH of the air decreases (ΔRH < 0). The rate of residue drying due to negative change in RH of the air is modeled using the following equations:

$$\frac{\Delta \text{residue } \theta_g}{\Delta t} = \begin{cases} k_2,\ \Delta RH < 0 \\ 0,\ \Delta RH \ge 0 \end{cases} \tag{5}$$

$$k_2 = c \cdot \text{T} \cdot \text{residue } \theta_g \tag{6}$$

where, $\frac{\Delta \text{residue } \theta_g}{\Delta t}$ is the rate of residue drying and is expressed as per unit

loss in residue θ_g per unit change in time (g H_2O g^{-1} dry matter h^{-1}), Δt is the change in time (h), k_2 is the rate constant (g H_2O g^{-1} dry matter h^{-1}) and c is a constant (0 to 1).

Transfer of water into the residue as a result of dew occurs once a day when there is no rain and the RH_t exceeds 85%. If the residue θ_g is below 2.5 g H_2O g^{-1} dry matter and residue biomass exceeds 1,500 kg ha^{-1}, dew deposition increases θ_g of cereal rye and crimson clover residues by 0.49 and 0.86 g H_2O g^{-1}dry matter, respectively, according to average values measured during the diurnal field studies. If RH_t decreases below 85% in the hour following dew deposition, the θ_g of cereal rye and crimson lover residues decreases by 0.2 and 0.4 g H_2O g^{-1}, dry matter, respectively, due to fast evaporation.

The rain effect on θ_g of cereal rye and crimson clover residues was modeled as a function of rainfall amount using the following equations derived from the rainfall simulation study (Fig. 3):

$$\text{residue}\,\theta_g = \begin{cases} 0.8523\cdot\left(1-exp^{(-0.9523\cdot RAIN)}\right)+2.9558\cdot\left(1-exp^{(-0.0583\cdot RAIN)}\right), rye \\ 1.6414\cdot\left(1-exp^{(-0.4351\cdot RAIN)}\right)+4.3623\cdot\left(1-exp^{(-0.0324\cdot RAIN)}\right), clover \end{cases} \quad (7)$$

where, *RAIN* is the total rain in mm (i.e., hourly rainfall + rain amount equivalent to the initial residue θ_g at the onset of rain event). The increase in residue θ_g due to a rain event was determined by subtracting the initial residue θ_g at the onset of rain from the final residue θ_g resulted from the total rain. For both residue types, the residue θ_g is dropped by 0.7 g H_2O g^{-1} dry matter due to drainage in the first hour following the cessation of the rain event.

3.7. Model calibration

The model was calibrated using data from a 41-h diurnal study conducted on Aug 15–16, 2018, as described above. Throughout the course of that study, air temperature and RH at a 2-m height fluctuated from 19 to 32 °C and from 46 to 99%, respectively. The $\psi_{residue}$ of cereal rye residue fluctuated from a maximum of −15.1 MPa (0.33 g H_2O g^{-1}dry matter) to a minimum −263.2 MPa (0.03 g H_2O g^{-1} dry matter). Fluctuations in crimson clover residue ranged from −19.2 MPa (0.37 g H_2O g^{-1}dry matter) to −174.4 MPa (0.05 g H_2O g^{-1} dry matter). Model simulations of $\psi_{residue}$ were compared with measured values and the drying and rewetting rates were calibrated to align model simulations with measured data. After calibration with the field measured data, the same value of k_1 was satisfactory for modeling residue rewetting for both residue species and hence, Eqs. (3) and (4) were modified in the final calibrated model as follows:

$$\frac{\Delta\text{residue}\,\theta_g}{\Delta t} = \begin{cases} k_1\cdot\psi_{gradient}, & \left(k_1\cdot\psi_{gradient}\right) < 0.01 \\ 0.02, & \left(k_1\cdot\psi_{gradient}\right) \rangle 0.01 \end{cases} \quad (8)$$

$$k_1 = \begin{cases} 0.0008, & \Delta RH > 0\ (AND)\ \psi_{gradient} < 30 \\ 0.0004, & \Delta RH > 0\ (AND)\ \psi_{gradient} > 30 \\ 0, & \Delta RH \le 0 \end{cases} \quad (9)$$

The value of k_2 for evaporation is a function of residue θ_g, air temperature, and the constant 0.01. The same rate of evaporation was applied to both residue species, and evaporation was set to no longer occur if θ_g falls below 0.04 g H_2O g^{-1} dry matter. Hence, Eqs. (5) and (6) were modified in the final calibrated model as follows:

$$\frac{\Delta\text{residue}\,\theta_g}{\Delta t} = \begin{cases} 0, \text{residue}\,\theta_g \le 0.04(\text{AND})\Delta\text{RH} \ge 0 \\ 0.001, \text{residue}\,\theta_g > 0.04(\text{AND})\Delta\text{RH} > -2.5 \\ 0.085, \text{residue}\,\theta_g > 0.04\,(\text{AND})\Delta\text{RH} \le -2.5(\text{AND})\,k_2 > 0.03 \\ k_2, \text{residue}\,\theta_g > 0.04(\text{AND})\Delta\text{RH} \le -2.5(\text{AND})\,k_2 < 0.03 \end{cases} \quad (10)$$

$$k_2 = 0.01\cdot\text{T}\cdot\text{residue}\ \theta_g \quad (11)$$

Additionally, a limit of −200 MPa was placed on $\psi_{residue}$ to prevent excessive decreases in residue θ_g. Considering the purpose of the model, strict accuracy in this very negative range is not required due to negligible (Thapa et al., 2021b) residue decomposition at $\psi_{residue}$ values below −60 MPa (Harris, 1981). Regression analysis provided a good fit of modeled vs. measured $\psi_{residue}$ data for cereal rye and crimson clover residues, providing NSE values of 0.90 and 0.92, respectively, and R^2 values of 0.96 and 0.99, respectively.

3.8. Model validation

Model performance was validated with five diurnal studies conducted from 2018 to 2019 (June 8 and September 5, 2018; July 24–25, August 28–29, and September 11–12, 2019), yielding a total of 39 measurements per residue species (Fig. 5 and 6). In general, the model simulated relatively well the observed diurnal patterns in $\psi_{residue}$. The simulated $\psi_{residue}$ reached its maximum value during early morning hours when the peak in RH was observed (Fig. 5 and 6). As RH decreased, the simulated $\psi_{residue}$ also decreased and reached values as low as −200 MPa in the afternoon. The RMSE value was 28.6 MPa for the combined data of both residues (Table 3).

It should be noted that this relatively high RMSE value was mainly due to differences between measured and observed values at very low water potentials (<−60 MPa), when microbial activity would be expected to be nil. In contrast, the RMSE value was 10.2 MPa ($N = 19$) for the $\psi_{residue}$ range of 0 to −20 MPa, which is where most microbial activity occurs. In general, in the higher $\psi_{residue}$ range of 0 to −20 MPa, the model tended to underpredict $\psi_{residue}$, with a mean difference of 7.9 MPa and a standard deviation of 6.5 MPa (with 17 simulated values being underpredictions and only two being slight overpredictions by 1 to 2 MPa). We believe this underprediction would likely lead to more realistic $\psi_{residue}$ under field conditions because $\psi_{residue}$ values in this study were measured with sample cups containing a 1-cm thick layer of surface residues, whereas in the field, cover crop residue layers are typically thicker than 1 cm and therefore, are likely to rewet to an average $\psi_{residue}$ that is more negative than the surface 1-cm layer.

Separate measurements taken during four of the diurnal studies ($N = 14$) were utilized to evaluate model performance when dewfall occurred. The model performed well as indicated by a RMSE of 3.3 MPa. As peak RH increased from 85 to 98%, residues gained progressively less moisture, a pattern also observed by Khanchi et al. (2018). There is potential to improve the simulation of dew deposition by implementing a dynamic increase in residue θ_g based on peak RH (or $\psi_{residue}$) at time of dewfall, rather than using a fixed value increase. Additional field measurements will be necessary to further validate model performance when simulating changes in $\psi_{residue}$ and residue θ_g immediately following dew deposition or rainfall, and to determine how these events affect residue moisture throughout the remainder of the diurnal period.

4. Conclusions

Our studies showed that the water release curves for cereal rye and crimson clover changed as decomposition progressed, and that parameters for the nonlinear model describing these curves could be estimated from residue lignin content. We also found that both types of residues rewetted rapidly when exposed to high relative humidity, and that the

Table 3
Model statistics in predicting surface residue water potential and water content in validation studies conducted in Georgia.

Residue	N	Residue Water Potential			Residue Water Content		
		RMSE (MPa)	NSE	R^2	RMSE (g H_2O g^{-1})	NSE	R^2
Ceral rye	39	26.3	0.86	0.88	0.06	0.72	0.81
Crimson clover	39	30.7	0.80	0.81	0.08	0.69	0.84
Both residues	78	28.6	0.83	0.84	0.07	0.71	0.82

amount of rainfall needed to reach maximum water content was lower for crimson clover than for cereal rye residues. Field observations showed a wide diurnal fluctuation in $\psi_{residue}$, which was due to residue rewetting under high RH during night and early morning hours, followed by drying during daylight hours. A simple model developed with the collected data simulates $\psi_{residue}$ with few parameters and a small set of input variables, namely initial water and lignin contents of the residue and hourly RH, air temperature, and precipitation. Validation studies indicated that the model simulates relatively well the observed diurnal patterns of $\psi_{residue}$ and θ_g of surface cereal rye and crimson clover residues. The small set of parameters and input data allows fast estimation of $\psi_{residue}$, which presents a practical advantage over more detailed models. Because $\psi_{residue}$ has a pronounced effect on microbial activity, this simple model may be incorporated into existing process-based decomposition models to estimate decomposition and N mineralization from cover crop residues remaining on the soil surface.

Credit Author Statement

Carson E. Dann: Conceptualization, Investigation, Writing-Original draft, Writing-Review & Editing. **M.L Cabrera**: Supervision, Conceptualization, Investigation, Writing-Original Draft, Writing-Review & Editing. **R. Thapa:** Investigation, Writing-Original Draft, Writing-Review & Editing. **S. Mirsky**: Funding acquisition, Conceptualization, Writing-Original Draft. **K. Tully:** Writing-Original Draft. **C. Reberg-Horton:** Funding acquisition, Conceptualization. **R. Hitchcock:** Software, Validation. and **F. Morari**: Conceptualization, Writing-Original Draft.

Declaration of Competing Interest

The authors declare that they have no known competing financial interests or personal relationships that could have appeared to influence the work reported in this paper.

Acknowledgements

This work was supported by NIFA AFRI Water CAP Grant 2018–68011–28372. The technical assistance of John Rema and Pietro Sica is gratefully acknowledged.

Supplementary materials

Supplementary material associated with this article can be found, in the online version, at doi:10.1016/j.ecolmodel.2021.109708.

References

Addiscott, T.M., Whitmore, A.P., 1987. Computer simulation of changes in soil mineral nitrogen and crop nitrogen during autumn, winter and spring. J. Agric. Sci. 109 (1), 141–157.
Barnett, R.D., Blount, A.R., Pfahler, P.L., Johnson, J.W., Buntin, G.D., Cunfer, B.M., 2002. Rye and triticale breeding in the South. UF University of Florida, IFAS Extension, SSAGR-42 1–3.
Bristow, K.L., Campbell, G.S., Papendick, R.I., Elliott, L.F., 1986. Simulation of heat and moisture transfer through a surface residue—Soil system. Agric. For. Meteorol. 36 (3), 193–214.
Cassity-Duffey, K., Cabrera, M., Rema, J., 2015. Ammonia volatilization from broiler litter: effect of soil water content 2and humidity. Soil Sci. Soc. Am. J. 79 (2), 543–550.
Coppens, F., Garnier, P., De Gryze, S., Merckx, R., Recous, S., 2006. Soil moisture, carbon and nitrogen dynamics following incorporation and surface application of labelled crop residues in soil columns. Eur. J. Soil Sci. 57 (6), 894–905.
Coppens, F., Garnier, P., Findeling, A., Merckx, R., Recous, S., 2007. Decomposition of mulched versus incorporated crop residues: modelling with PASTIS clarifies interactions between residue quality and location. Soil Biol. Biochem. 39 (9), 2339–2350.
Douglas, C.L., Rickman, R.W., 1992. Estimating crop residue decomposition from air temperature, initial nitrogen content, and residue placement. Soil Sci. Soc. Am. J. 56 (1), 272–278.
Dunlop, M.W., McAuley, J., Blackall, P.J., Stuetz, R.M., 2016. Water activity of poultry litter: relationship to moisture content during a grow-out. J. Environ. Manage. 172, 201–206.
Findeling, A., Chanzy, A., De Louvigny, N., 2003. Modeling water and heat flows through a mulch allowing for radiative and long-distance convective exchanges in the mulch. Water Resour. Res. 39 (9).
Findeling, A., Garnier, P., Coppens, F., Lafolie, F., Recous, S., 2007. Modelling water, carbon and nitrogen dynamics in soil covered with decomposing mulch. Eur. J. Soil Sci. 58 (1), 196–206.
Young, M.H., Sisson, J.B., 2002. Tensiometry. In: Dane, J.H., Topp, G.C. (Eds.), Methods of Soil Analysis, Part 4 – Physical Methods. Soil Science Society of America, Madison, Wisconsin, USA, pp. 575–578.
Harris, R.F., .1981. Effect of water potential on microbial growth and activity. In Parr, J. F, Gardner. W.R. (Eds). Water potential relations in soil microbiology. Soil Science Society of America Special Publications Volume 9, pp. 23.95.
Horwath, W., 2015. Carbon Cycling: the dynamics and formation of organic matter. In: Paul, E.A. (Ed.), Soil microbiology, Ecology and Biochemistry. Academic Press.
Iqbal, A., Beaugrand, J., Garnier, P., Recous, S., 2013. Tissue density determines the water storage characteristics of crop residues. Plant Soil 367 (1–2), 285–299.
Khanchi, A., Birrell, S., Mitchell, R.B., 2018. Modelling the influence of crop density and weather conditions on field drying characteristics of switchgrass and maize stover using random forest. Biosyst. Eng. 169, 71–84.
Kieft, T.L., 1987. Microbial biomass response to a rapid increase in water potential when dry soil is wetted. Soil Biol. Biochem. 19 (2), 119–126.
Kissel, D.E., Cabrera, M.L., Vaio, N., Craig, J.R., Rema, J.A., Morris, L.A., 2004. Rainfall timing and ammonia loss from urea in a loblolly pine plantation. Soil Sci. Soc. Am. J. 68 (5), 1744–1750.
Magan, N., Lynch, J.M., 1986. Water potential, growth and cellulolysis of fungi involved in decomposition of cereal residues. Microbiology 132 (5), 1181–1187.
Maloney, T.C., Paulapuro, H., 1999. The formation of pores in the cell wall. J. Pulp Pap. Sci. 25 (12), 430–436.
Manstretta, V., Rossi, V., 2015. Modelling the effect of weather on moisture fluctuations in maize stalk residues, an important inoculum source for plant diseases. Agric. For. Meteor. 207, 83–93.
Manzoni, S., Schimel, J.P., Porporato, A., 2012. Responses of soil microbial communities to water stress: results from a meta-analysis. Ecology 93 (4), 930–938.
Milliken, G.A., Debruin, R.L., 1978. A procedure to test hypotheses for nonlinear models. Commun. Stat.-Theory Methods 7, 65–79.
Moriasi, D.N., Arnold, J.G., Van Liew, M.W., Bingner, R.L., Harmel, R.D., Veith, T.L., 2007. Model evaluation guidelines for systematic quantification of accuracy in watershed simulations. Trans. ASABE 50 (3), 885–900.
Moyano, F.E., Manzoni, S., Chenu, C., 2013. Responses of soil heterotrophic respiration to moisture availability: an exploration of processes and models. Soil Biol. Biochem. 59, 72–85.
Myrold, D.D., Elliott, L.F., Papendick, R.I., Campbell, G.S., 1981. Water Potential-Water Content Characteristics of Wheat Straw. Soil Sci. Soc. Am. J. 45 (2), 329–333.
Nash, J.E., Sutcliffe, J.V., 1970. River flow forecasting through conceptual models part I—a discussion of principles. J. Hydrol. (Amst) 10 (3), 282–290.
Parr, J.F., Papendick, R.I., 1978. Factors affecting the decomposition of crop residues by microorganisms. Crop Residue Manage. Syst. 101–129.
Quemada, M., Cabrera, M., 1995a. Carbon and nitrogen mineralized from leaves and stems of four cover crops. Soil Sci. Soc. Am. J. (2), 471.
Quemada, M., Cabrera, M.L., 1995b. CERES-N model predictions of nitrogen mineralized from cover crop residues. Soil Sci. Soc. Am. J. 59 (4), 1059–1065.
Quemada, M., Cabrera, M.L., McCracken, D.V., 1997. Nitrogen release from surface-applied cover crop residues: evaluating the CERES-N submodel. Agron. J. 89 (5), 723–729.
Quemada, M., Cabrera, M.L., 2002. Characteristic moisture curves and maximum water content of two crop residues. Plant Soil 238 (2), 295–299.
Reicosky, D.C., 2015. Conservation tillage is not conservation agriculture. J. Soil Water Conserv. 70 (5), 103A–108A.
SAS Institute Inc., 2015. SAS/STAT 9.4 User's Guide. SAS Institute Inc., Cary, NC.
SAS Institute Inc., 2019. JMP® 15 Basic Analysis. SAS Institute Inc., Cary, NC.
Sain, P., Broadbent, F.E., 1975. Moisture Absorption, Mold Growth, and Decomposition of Rice Straw at Different Relative Humidities. Agron. J. 67 (6), 759–762.
Shane, M.W., McCully, M.E., Canny, M.J., 2000. The vascular system of maize stems revisited: implications for water transport and xylem safety. Ann. Bot. 86 (2), 245–258.
Singh, D.P., Backhouse, D., Kristiansen, P., 2009. Interactions of temperature and water potential in displacement of Fusarium pseudograminearum from cereal residues by fungal antagonists. Biol. Control 48 (2), 188–195.
Snow, D., Crichton, M.H.G., Wright, N.C., 1944. Mould deterioration of feeding-stuffs in relation to humidity of storage: part II. The water uptake of feeding-stuffs at different humidities. Ann. Appl. Biol. 31 (2), 111–116.
Soil Science Glossary Terms Committee, 2008. Glossary of Soil Science Terms. Soil Science Society of America, Madison, WI.
Strømdahl, K., 2000. Water sorption in wood and plant fibres. PhD Thesis. Department of Structural Engineering and Materials, Technical University of Denmark.
Stroo, H.F., Bristow, K.L., Elliott, L.F., Papendick, R.I., Campbell, G.S., 1989. Predicting rates of wheat residue decomposition. Soil Sci. Soc. Am. J. 53 (1), 91–99.
Thapa, R., Tully, K., Cabrera, M.L., Dann, C., Schomberg, H.H., Timlin, D., Gaskin, J., Reberg-Horton, C., Miskly, S.B., 2021b. Cover crop residue moisture content controls diurnal variations in surface residue decomposition. Agric. For. Meteorol. 308-308, 108537.
Thapa, R., Tully, K., Cabrera, M.L., Dann, C., Schomberg, H.H., Timlin, D., Reberg-Horton, C., Gaskin, J., Davis, B.W., Miskly, S.B., 2021a. Effects of moisture and

temperature on C and N mineralization from surface-applied cover crop residues. Biol. Fertil. Soils. 57 (4), 485–498. https://doi.org/10.1007/s00374-021-01543-7.
Van Soest, P.J., 1963a. Use of detergents in the analysis of fibrous feeds. 1. Preparation of fiber residues of low nitrogen content. J. Assoc. Off. Agric. Chem. 46, 825–829.
Van Soest, P.J., 1963b. Use of detergents in the analysis of fibrous feeds. 2. A rapid method for the determination of fiber and lignin. J. Assoc. Off. Agric. Chem. 46, 829–835.
Woodruff, L.K., Kissel, D.E., Cabrera, M.L., Habteselassie, M.Y., Hitchcock, R., Gaskin, J., Rema, J., 2018. A Web-Based Model of N Mineralization from Cover Crop Residue Decomposition. Soil Sci. Soc. Am. J. 82 (4), 983–993.